Electronic Supplementary Material (ESI) for RSC Advances.

Supporting Information

Fabrication and Electrochemical Performance of Novel Hollow Microporous Carbon Nanospheres

Luyi Chen, [a,b] **Yeru Liang,***[a] **Hao Liu,** [a] **Weicong Mai,** [a] **Zhiyong Lin,*** [b] **Hongji Xu,** [a] **Ruowen Fu** [a] **and Dingcai Wu*** [a]

[a] *Materials Science Institute, PCFM Laboratory, School of Chemistry and Chemical Engineering, Sun Yat-sen University, Guangzhou 510275, P. R. China*

[b] *Department of Material Science and Engineering, Huaqiao University, Xiamen, 361021, P. R. China*

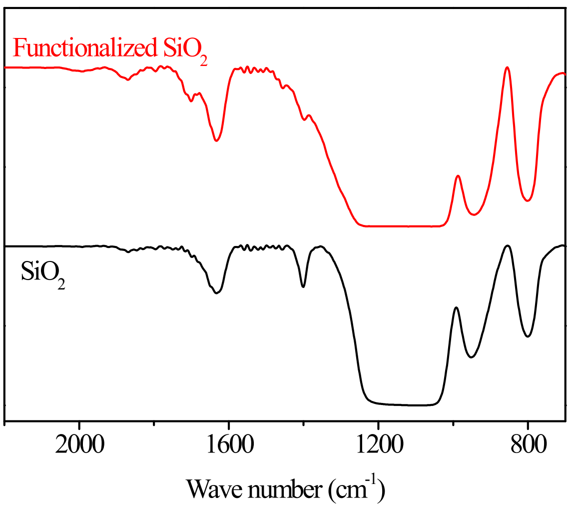

Fig. S1 FTIR spectrum of SiO_2 nanoparticles and functionalized SiO_2 nanoparticles.

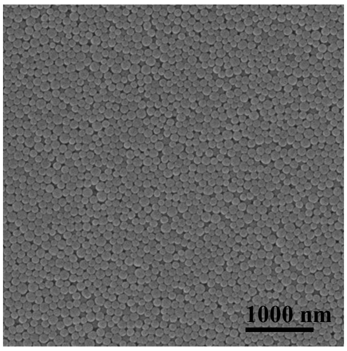

Fig. S2 SEM image of SiO_2 nanoparticles.

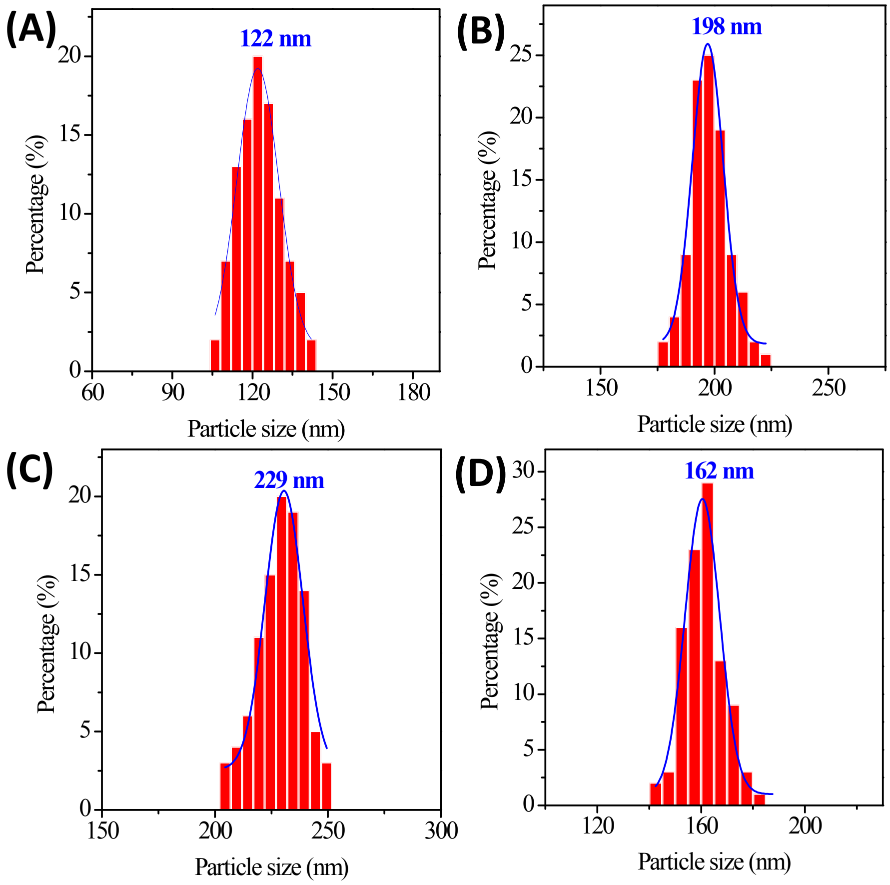

Fig. S3 Particle size distribution from SEM image analysis of (A) SiO_2 nanoparticles, (B) SiO_2@PS nanospheres, (C) SiO_2@*x*PS-24 nanospheres and (D) HCMNS-24.

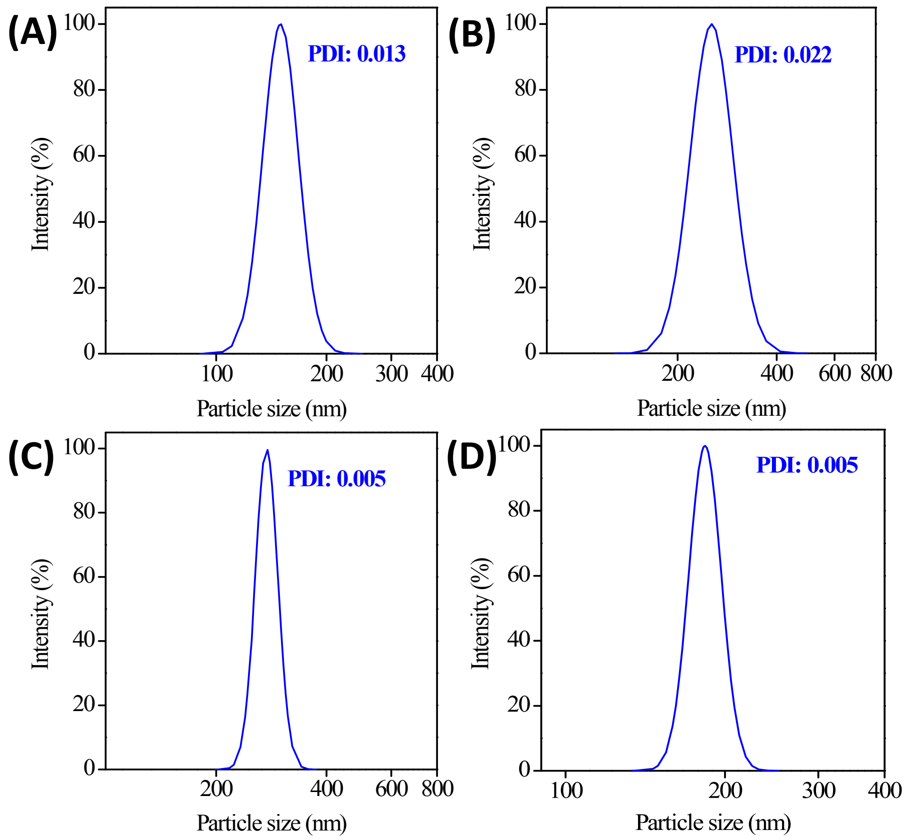

Fig. S4 DLS curves of (A) functionalized SiO_2 nanoparticles, (B) SiO_2@PS nanospheres, (C) SiO_2@*x*PS-24 nanospheres and (D) HCMNS-24.

(1) Formation of carbocation $^{+}CCl_3$

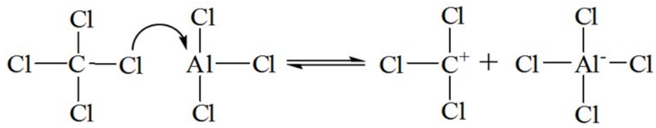

(2) Formation of -CCl_2- crosslinking bridges

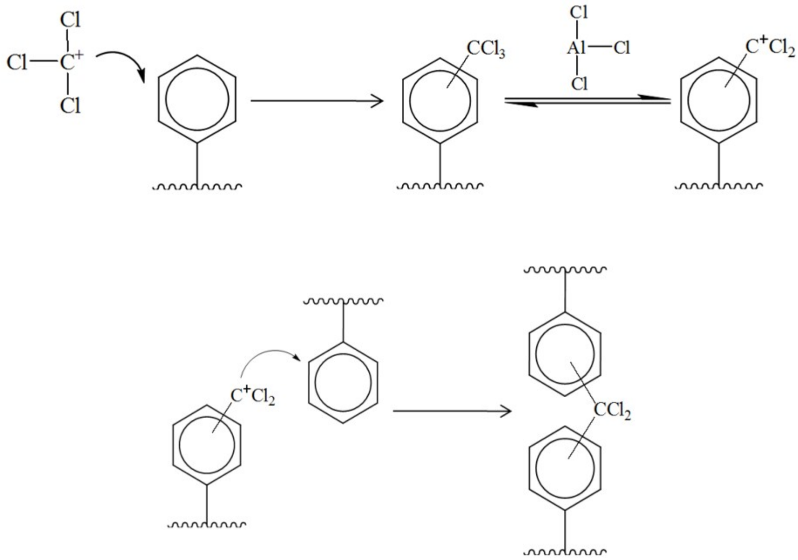

(3) Formation of -CO- crosslinking bridges

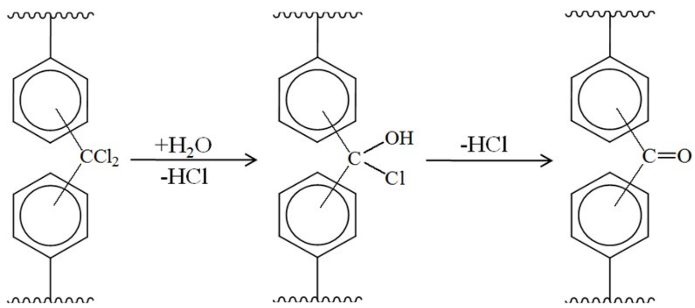

Fig. S5 Formation mechanism of –CO– crosslinking bridges based on the Friedel-Crafts reaction of polystyrene chain and carbon tetrachloride and subsequent hydrolysis. [S1]

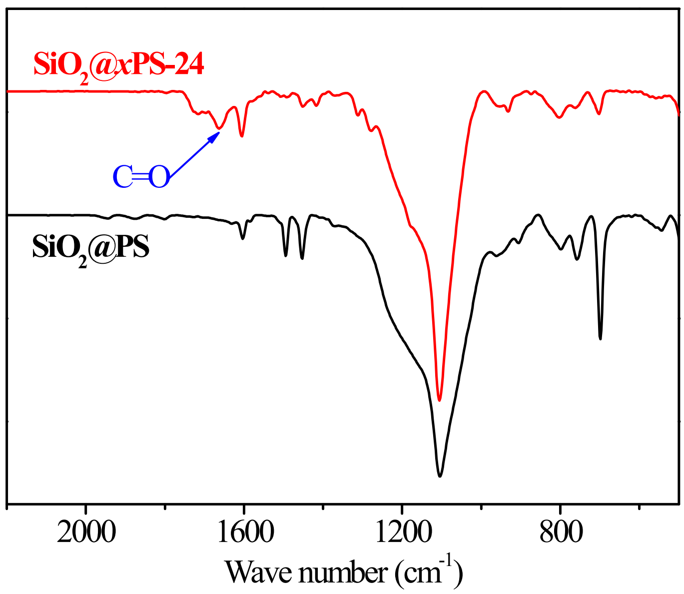

Fig. S6 FTIR spectrum of SiO_2@PS nanospheres and SiO_2@*x*PS-24 nanospheres.

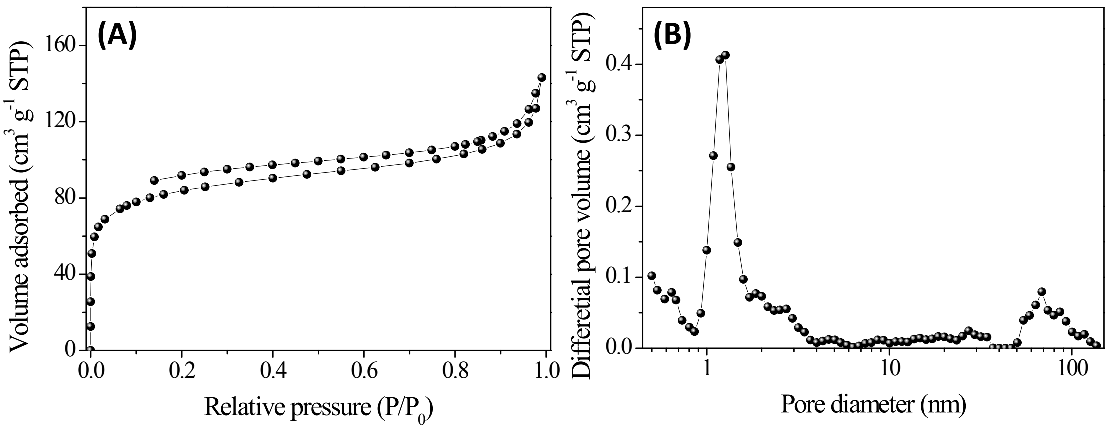

Fig. S7 (A) N_2 adsorption-desorption isotherm and (B) DFT pore size distribution of SiO_2@*x*PS-24.

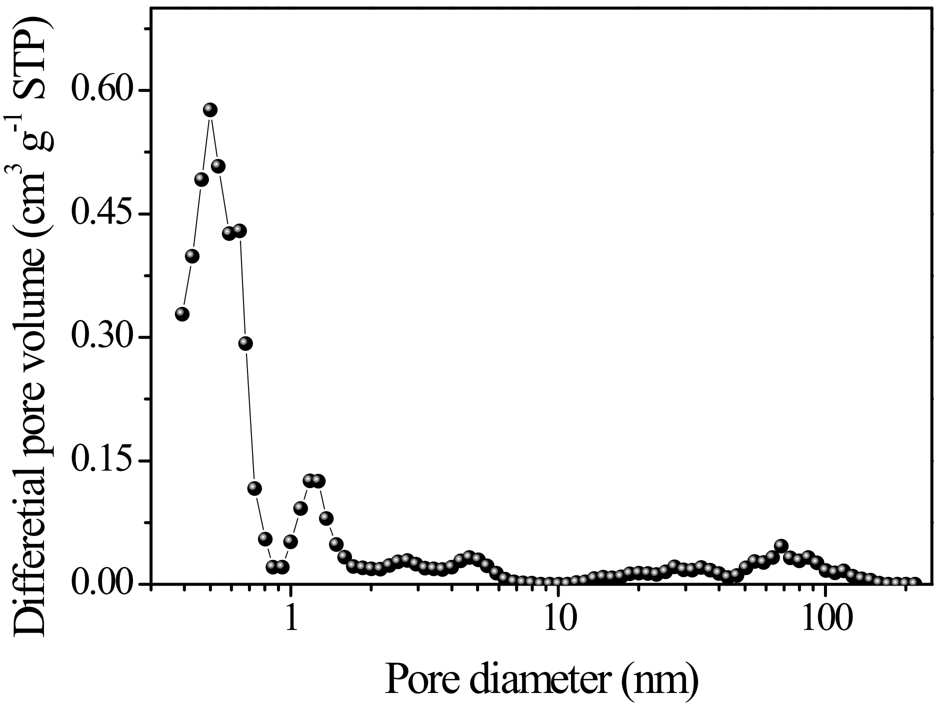

Fig. S8 DFT pore size distribution of carbonized SiO_2@*x*PS-24.

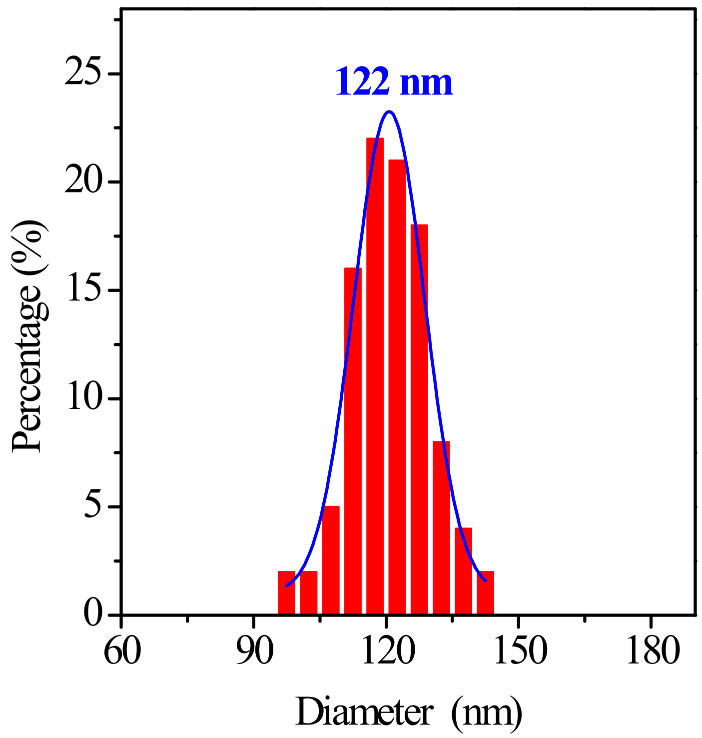

Fig. S9 Core size distribution of HMCNS-24 based on TEM image analysis.

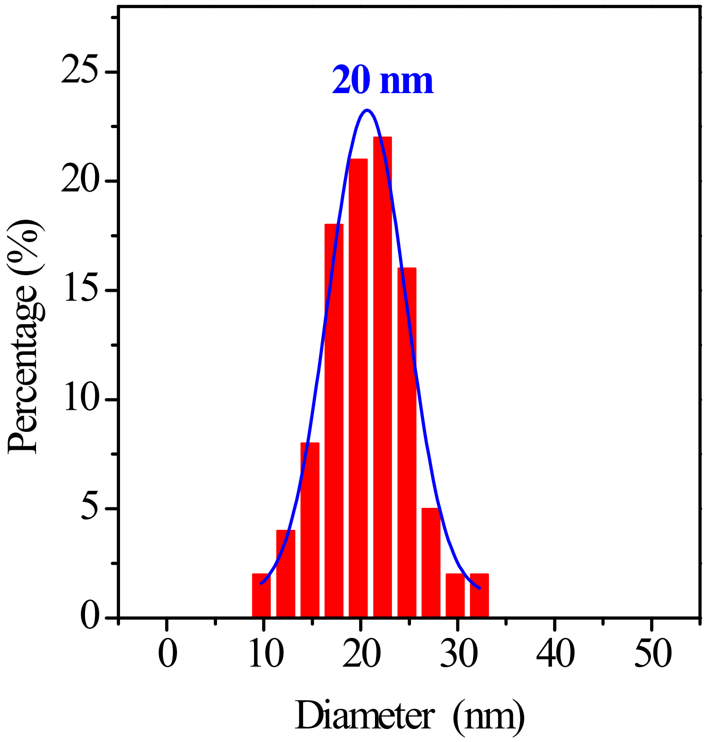

Fig. S10 Shell thickness distribution of HMCNS-24 based on TEM image analysis.

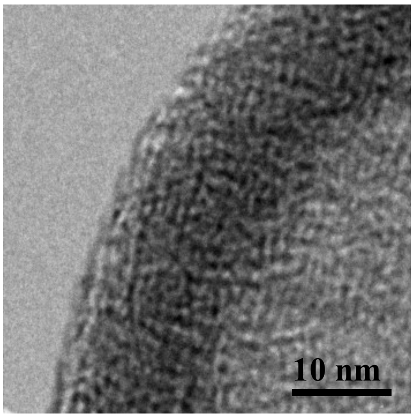

Fig. S11 High-resolution TEM image of HCMNS-24.

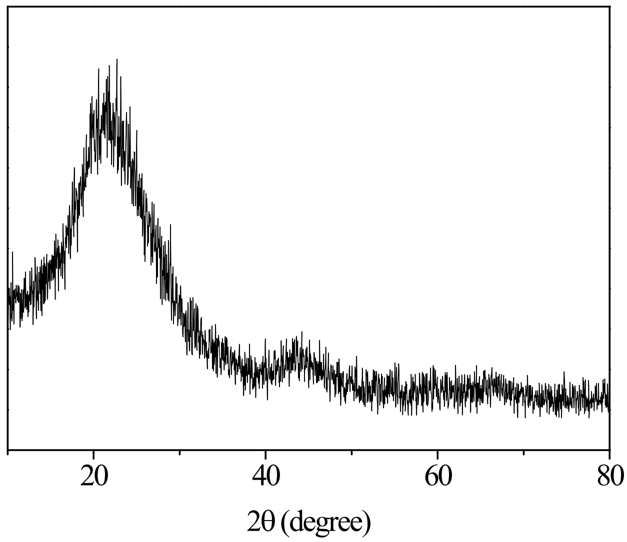

Fig. S12 XRD pattern of HMCNS-24.

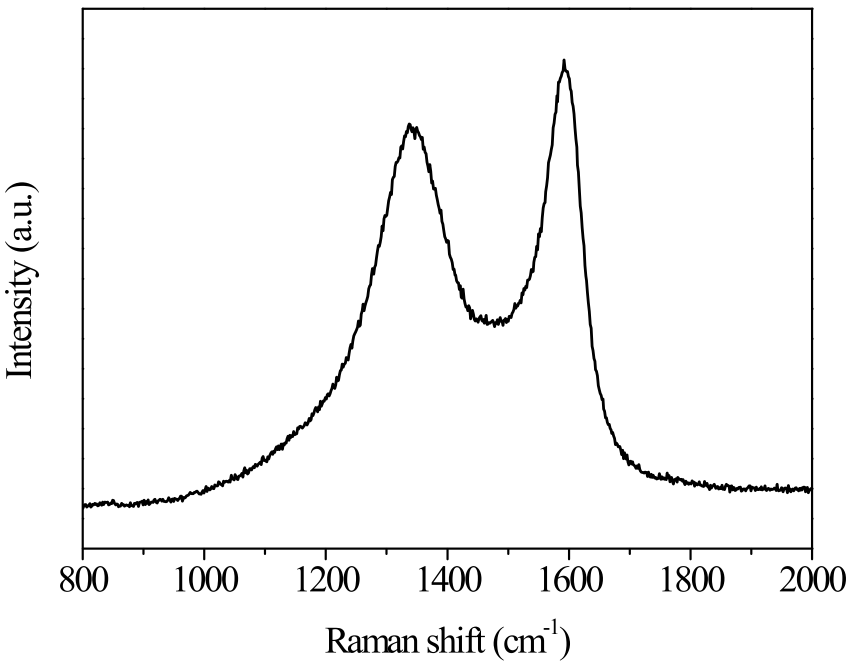

Fig. S13 Raman spectrum of HMCNS-24.

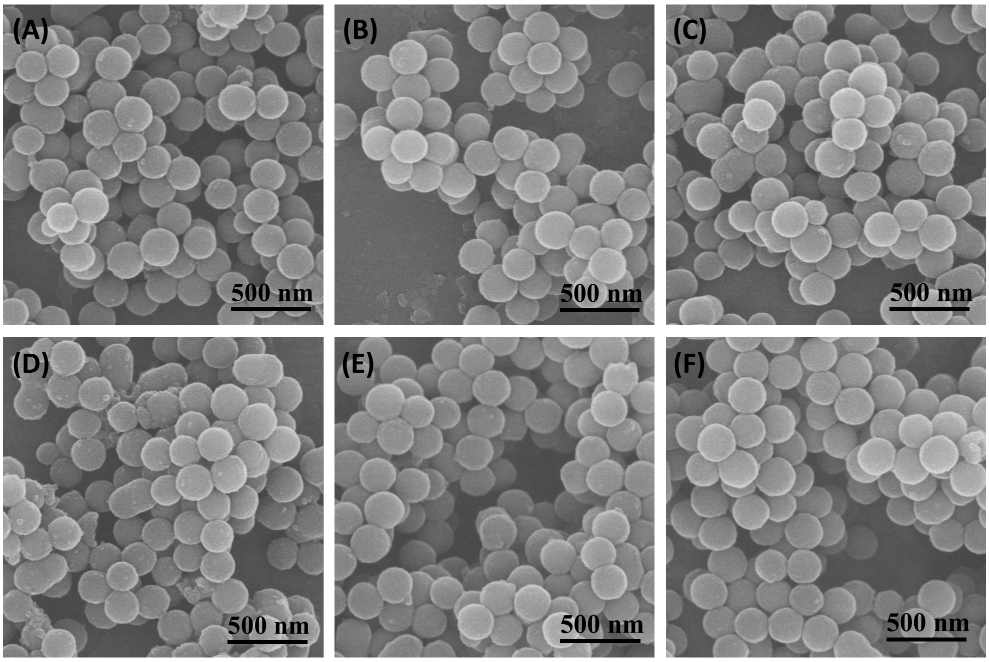

Fig. S14 SEM images of SiO_2@*x*PS nanospheres under different hypercrosslinking reaction times: (A) 0.25 h, (B) 1 h, (C) 2 h, (D) 8 h, (E) 24 h and (F) 48 h.

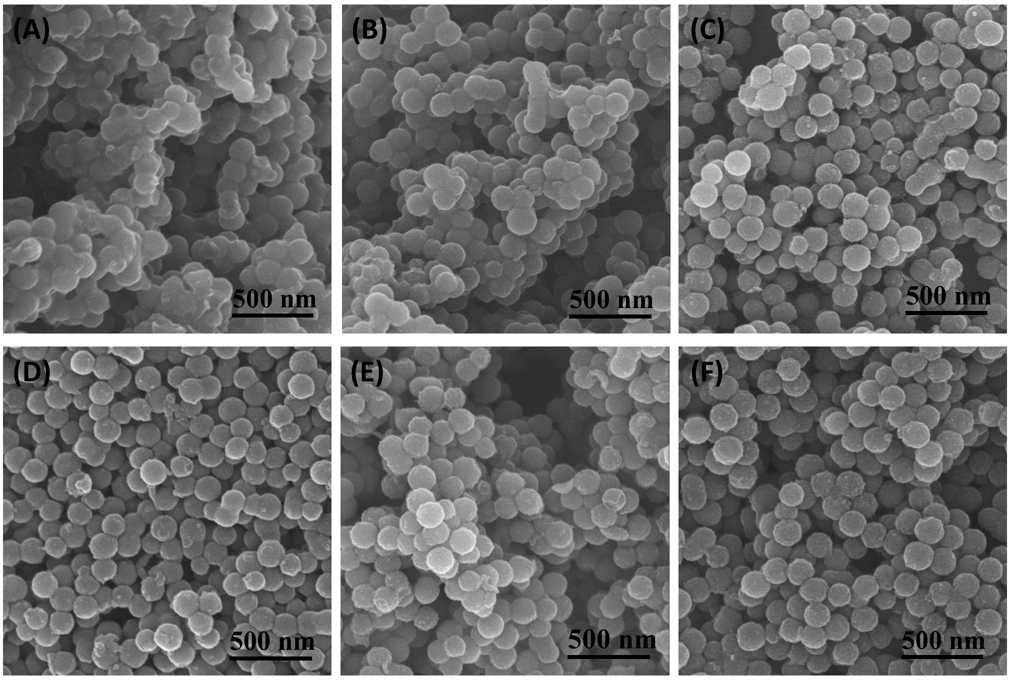

Fig. S15 SEM images of (A) HCMNS-0.25, (B) HMCNS-1, (C) HMCNS-2, (D) HMCNS-8, (E) HMCNS-24 and (F) HMCNS-48.

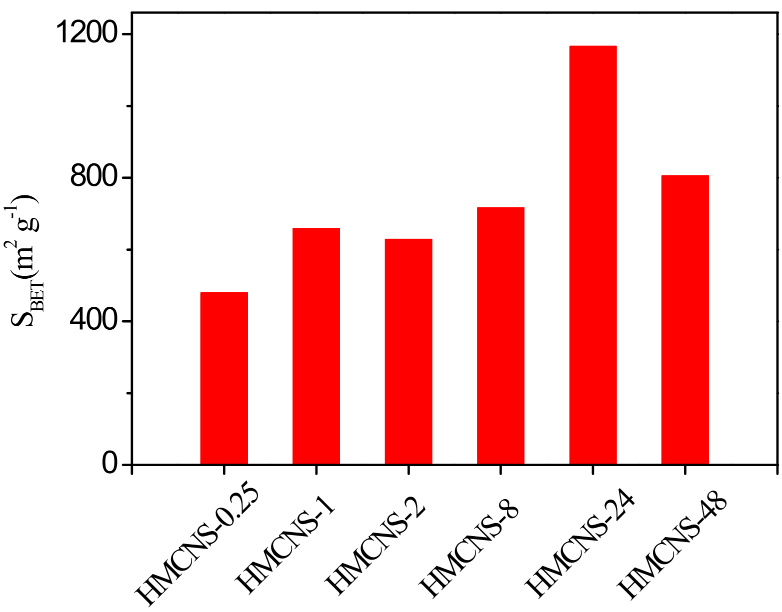

Fig. S16 BET surface areas of HCMNS-0.25, HMCNS-1, HMCNS-2, HMCNS-8, HMCNS-24 and HMCNS-48.

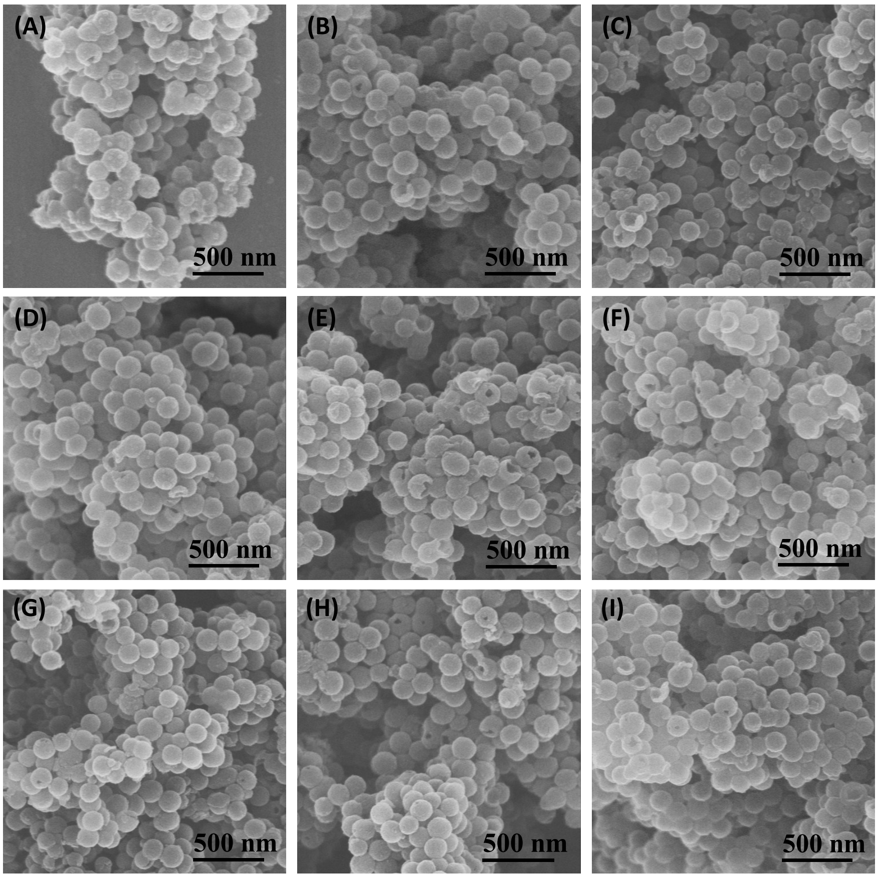

Fig. S17 SEM images of HMCNSs obtained at various carbonization conditions, including (A) 700 ˚C, (B) 800 ˚C and (C) 1000 ˚C at 5 ˚C min^{-1} for 3 h; (D) 1 h, (E) 2 h, (F) 10 h at 900 ˚C with 5 ˚C min^{-1}; (G) 1 ˚C min^{-1}, (H) 2 ˚C min^{-1} and (I) 10 ˚C min^{-1} at 900 ˚C for 3 h.

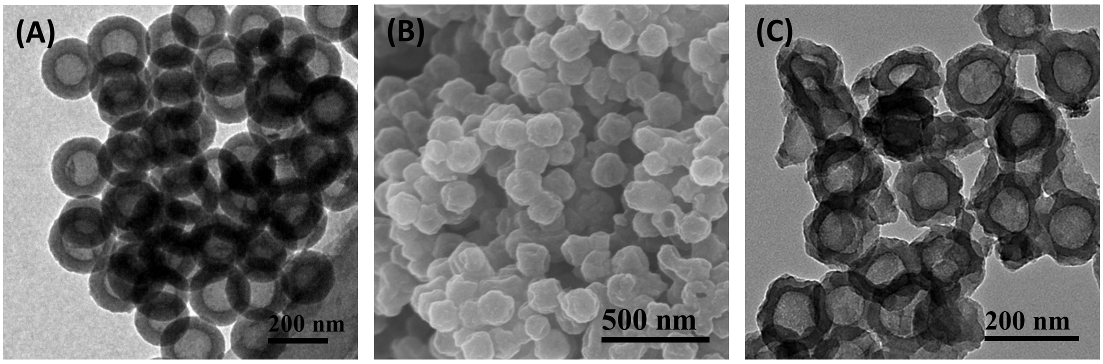

Fig. S18 (A) TEM image of SiO_2@*x*PS-24 without silica cores, (B) SEM and (C) TEM images of control carbon sample.

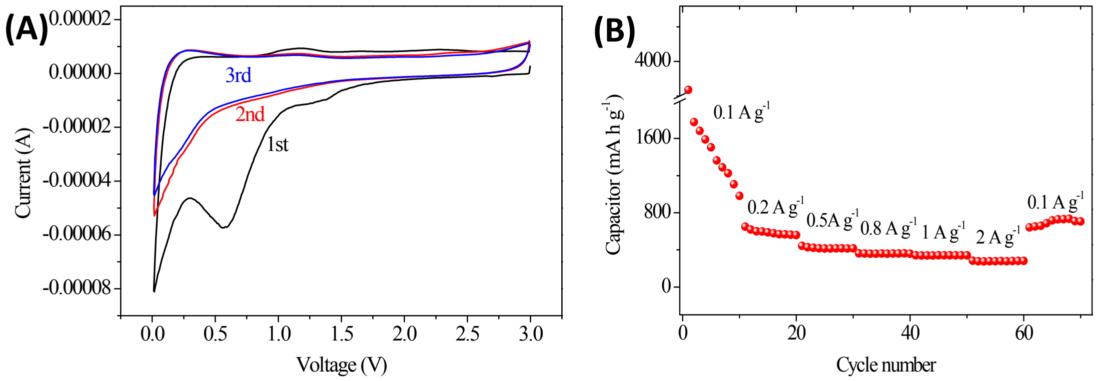

Fig. S19 (A) CV plots for the first 3 cycles at the scan rate of 0.1 mV s^{-1}, (B) rate performances at different current densities of HMCNS-24.

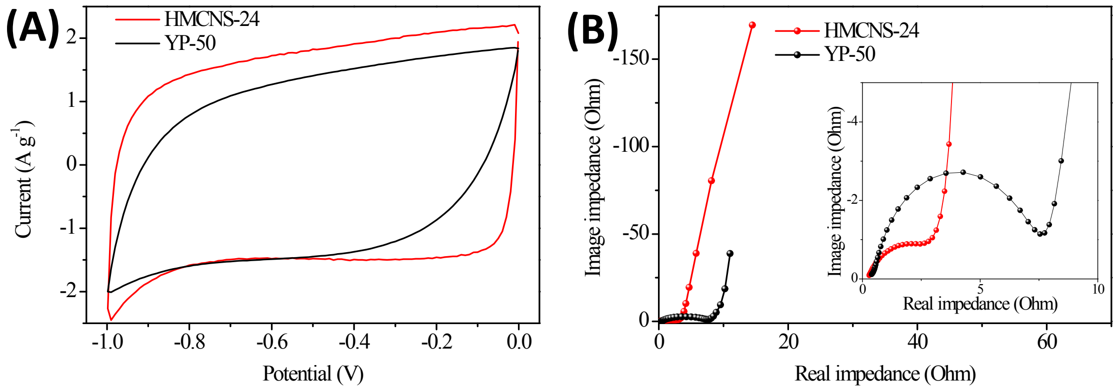

Fig. S20 (A) CV curves at the sweep rate of 25 mV s^{-1}, (B) Nyquist plots for HMCNS-24 and YP-50.

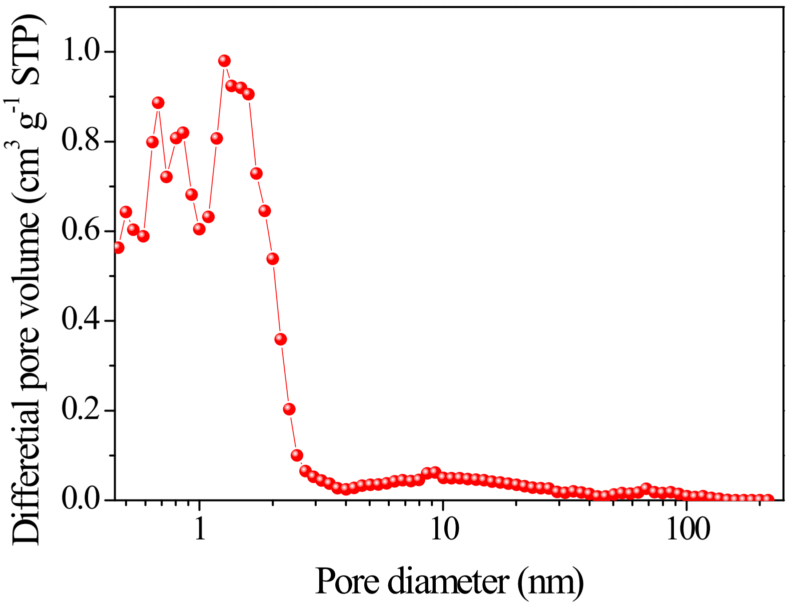

Fig. S21 DFT pore size distribution of YP-50. From the DFT pore size distribution curve, it can be clearly seen that YP-50 is microporous carbon material.

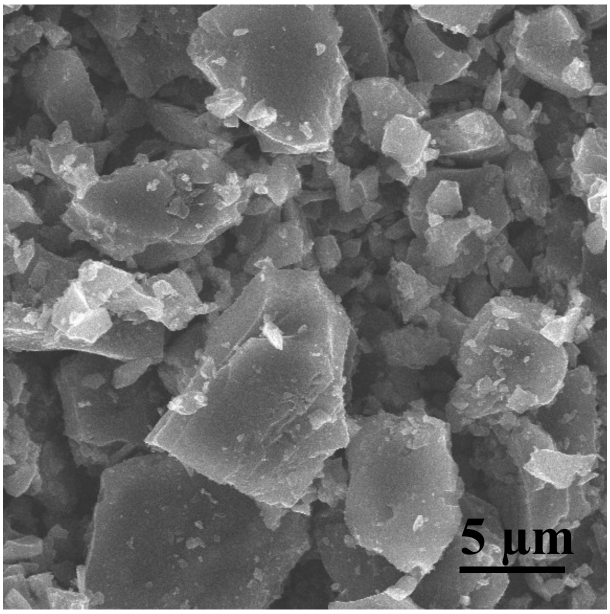

Fig. S22 SEM image of YP-50. From SEM image, it can be seen that the diameter of carbon particle of YP-50 is mainly micron-scale.

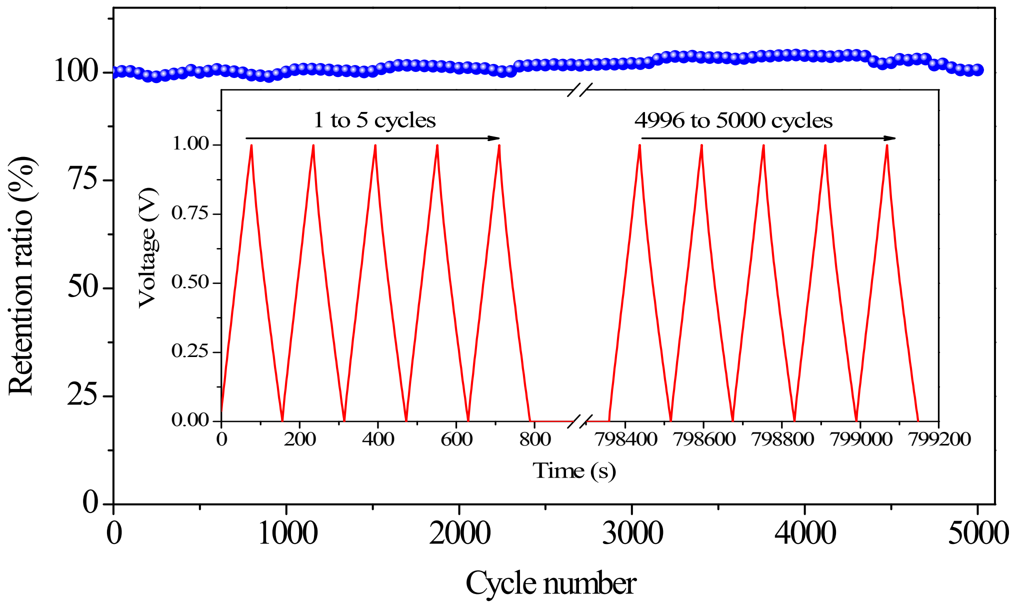

Fig. S23 Long-term cycling stability over 5,000 cycles for HMCNS-24 at a current density of 1A g^{-1}; the inset shows the charging-discharging curves for the first and last five cycles.

Table S1 Pore structure parameters of typical samples.

Sample	S_{BET} (m^2 g^{-1})	S_{ext} (m^2 g^{-1})	S_{mic} (m^2 g^{-1})	V_t (cm^3 g^{-1})	V_{mic} (cm^3 g^{-1})
SiO_2@*x*PS-24	287	127	160	0.22	0.07
carbonized SiO_2@*x*PS-24	396	317	79	0.24	0.15
HMCNS-24	1166	583	583	1.36	0.27
YP-50	1396	1022	374	0.73	0.47

Table S2 Comparison of the cycling performance of hollow or solid carbon spheres as lithium-ion battery anodes in the references.

Sample		**Stable capacity (mA h g^{-1})**	**Current density (mA g^{-1})**	**Cycle number**	**Voltage range (V)**	**Ref.**
Hollow carbon spheres	**HMCNS**	**620**	**100**	**50**	**0-3**	**This work**
	Hollow carbon nanospheres	310	372	200	0-3	S2
	Carbon hollow particles	330	0.15 (mA cm^{-2})	5	0-1.5	S3
	Hollow carbon nanoparticles	443	50	75	0-3	S4
	Interconnected hollow carbon nanospheres	630	37.2	50	0-3	S5
	Hollow graphitic carbon nanospheres	391	37.2	60	0-3	S6
	Nanographene-constructed hollow carbon spheres	600	74.4	30	0-3	S7
	Hollow graphene oxide spheres	485	0.2 (mA cm^{-2})	30	0-2.5	S8
	Hard carbon nano-spherules	475	0.2 (mA cm^{-2})	20	-0.15-2.5	S9
Solid carbon spheres	Carbon nanospheres	420	60	60	0-3	S10
	Nitrogen-doped carbon nanoparticles	423	37.2	100	0-3	S11
	Porous carbon microspheres	450	50	50	0-2	S12

Table S3 Comparison of the capacitance retention ratios of HMCNS-24 and other carbon spheres as high-performance supercapacitor electrode in the references.

Sample		Current density	Capacitance retention ratio		
			Ref.		HMCNS-24 (This work)
Hollow carbon spheres	Hollow carbon spheres	1-20 A g^{-1}	75.7 %	S13	**81.2 %**
	N- and O-doped hollow carbon spheres	0.5-5 A g^{-1}	42.9 %	S14	**87.8 %**
	Hollow carbon spheres	0.2-1 A g^{-1}	60.6 %	S15	**91.1 %**
	Hierarchical porous carbon hollow-pheres	0.5-10 A g^{-1}	73 %	S16	**81.9 %**
	Hollow carbon nanospheres	0.05-10 A g^{-1}	81.8 %	S17	**65.0 %**
	Hollow carbon nanospheres	0.1-10 A g^{-1}	79.0 %	S18	**73.4 %**
	Nitrogen-rich hollow porous carbon	0.5-10 A g^{-1}	66.1 %	S19	**81.9 %**
	N-doped hollow carbon spheres	0.5-10 A g^{-1}	55.6 %	S20	**81.9 %**
Solid carbon spheres	Solid carbon nanospheres	0.1-10 A g^{-1}	75.7 %	S18	**73.4 %**
	Mesoporous carbon spheres	0.5-30 A g^{-1}	70.2 %	S21	**65.2 %**
	Monodisperse Carbon Spheres	1-50 mV s^{-1}	68.4 %	S22	**81.3 %**
Activated carbon	YP-50	0.05-10 A g^{-1}	23.6 %	This work	**65.0 %**

References

(S1) Wu, D. C.; Nese, A.; Pietrasik, J.; Liang, Y. R.; He, H. K.; Kruk, M.; Huang, L.; Kowalewski, T.; Matyjaszewski, K. *Acs Nano* **2012**, *6*, 6208.

(S2) Tang, K.; White, R. J.; Mu, X. K.; Titirici, M. M.; van Aken, P. A.; Maier, J. *ChemSusChem* **2012**, *5*, 400.

(S3) Zhang, H. J.; Xu, H. F.; Zhao, C. *Mater. Chem. Phys.* **2012**, *133*, 429.

(S4) Yang, Z. C.; Zhang, Y.; Kong, J. H.; Wong, S. Y.; Li, X.; Wang, J. *Chem. Mater.* **2013**, *25*, 704.

(S5) Han, F. D.; Bai, Y. J.; Liu, R.; Yao, B.; Qi, Y. X.; Lun, N.; Zhang, J. X. *Adv. Energy Mater.* **2011**, *1*, 798.

(S6) Feng, J.; Li, F.; Bai, Y. J.; Han, F. D.; Qi, Y. X.; Lun, N.; Lu, X. F. *Mater. Chem. Phys.* **2013**, *137*, 904.

(S7) Yang, S. B.; Feng, X. L.; Zhi, L. J.; Cao, Q. A.; Maier, J.; Mullen, K. *Adv. Mater.* **2010**, *22*, 838.

(S8) Guo, P.; Song, H. H.; Chen, X. H. *J. Mater. Chem.* **2010**, *20*, 4867.

(S9) Hu, J.; Li, H.; Huang, X. *Solid State Ionics*, **2007**, *178*, 265-271.

(S10) Wang, Y.; Su, F. B.; Wood, C. D.; Lee, J. Y.; Zhao, X. S. *Ind. Eng. Chem. Res.* **2008**, 47, 2294.

(S11) Bhattacharjya, D.; Park, H. Y.; Kim, M. S.; Choi, H. S.; Inamdar, S. N.; Yu, J. S. *Langmuir* **2014**, *30*, 318.

(S12) Zhang, L.; Zhang, M. J.; Wang, Y. H.; Zhang, Z. L.; Kan, G. W.; Wang, C. G.; Zhong, Z. Y.; Su, F. B. *J. Mater. Chem. A* **2014**, *2*, 10161.

(S13) Fang, X. L.; Zang, J.; Wang, X. L.; Zheng, M. S.; Zheng, N. F. *J. Mater. Chem. A*, **2014**, 2, 6191.

(S14) Yuan, C.Q.; Liu, X. H.; Jia, M. Y.; Luo, Z. X.; Yao, J. N. *J. Mater. Chem. A* **2015**, 3, 3409.

(S15) Chen, X.; Kierzek, K.; Cendrowski, K.; Pelech, I.; Zhao, X.; Feng, J.; Kalenczuk, R.; Tang, T.; Mijowska, E. *Colloid. Surface. A* **2012**, *396*, 246.

(S16) Han, Y.; Dong, X. T.; Zhang, C.; Liu, S. X. *J. Power Sources* **2012**, 211, 92.

(S17) Xu, F.; Tang, Z. W.; Huang, S. Q.; Chen, L. Y.; Liang, Y. R.; Mai, W. C.; Zhong, H.; Fu, R. W.; Wu, D. C. *Nat. Comm.* **2015**, 6, 7221.

(S18) Wang, C. W.; Wang, Y.; Graser, J.; Zhao, R.; Gao, F.; O'Connell, M. J. *ACS nano* 2013, 7, 11156.

(S19) Liu, X.H.; Zhou, L.; Zhao, Y. Q.; Bian, L.; Feng, X. T.; Pu, Q. S. *ACS Appl. Mater. Interfaces* **2013**, 5, 10280.

(S20) Han, J. P.; Xu, G. Y.; Ding, B.; Pan, J.; Dou, H.; MacFarlane, D. R. *J. Mater. Chem. A* **2014**, 2, 5352.

(S21) Li, Q.; Jiang, R. R.; Dou, Y. Q.; Wu, Z. X.; Huang, T.; Feng, D.; Yang, J. P.; Yu, A. S.; Zhao, D. Y. *CARBON*, **2011**, 49, 1248.

(S22) Tanaka, S.; Nakao, H.; Mukai, T.; Katayama, Y.; Miyake, Y. *J. Phys. Chem. C* **2012**, 116, 26791.